Pergamon

Bioorganic & Medicinal Chemistry 6 (1998) 1491–1500

BIOORGANIC & MEDICINAL CHEMISTRY

New Insights into the Conformational Requirements of B2 Bradykinin Antagonism

Marta Filizola,[a,b] Oriol Llorens,[b] Maria Cartení-Farina[a] and Juan J. Perez[b,*]

[a]*Centro di Ricerca Interdipartimentale di Scienze Computazionali e Biotecnologiche (CRISCEB), Seconda Universitá degli Studi di Napoli, Via Costantinopoli, 16, 80138 Napoli, Italy*

[b]*Dept. d'Enginyeria Quimica, UPC, ETS d'Enginyers Industrials, Av. Diagonal, 647, 08028 Barcelona, Spain*

Received 25 September 1997; accepted 27 February 1998

Abstract—The conformational profiles of a selected group of a new series of small linear and cyclic penta- and hexapeptides, inspired on the C-terminal segment of second-generation bradykinin (BK) antagonists, were independently computed in order to assess the chemical and geometrical requirements necessary for BK antagonism. Specifically, four cyclic peptides: cyclo-(Gly-Thi-D-Tic-Oic-Arg), cyclo-(Gly-Ala-D-Tic-Oic-Arg), cyclo-(Abu-Ala-Ser-D-Tic-Oic-Arg), cyclo-(Abu-D-Phe-Ala-D-Tic-Oic-Arg), and a linear peptide: Thi-Ser-D-Tic-Oic-Arg were selected for the present study. The first three BK analogs are capable to antagonize kinin-induced rabbit jugular vein and rabbit aorta smooth muscle contraction, while last two show no detectable affinity for the BK B2 receptor. The conformational space of the five peptides was thoroughly explored using simulated annealing (SA) in an iterative fashion as sampling technique. The bioactive conformation was assessed by pairwise cross comparisons between each of the unique low energy conformations found for each of the different peptides studied within a 5 kcal/mol threshold in respect to the global minimum. The conformational profile of the highly potent BK antagonist HOE-140, computed in an independent study, was also used in conjunction with the bioactive form assessed in the present study, to propose a pharmacophore that includes the stereochemical requirements for B2 BK antagonism.

Introduction

Bradykinin (BK) is a linear nonapeptide hormone of sequence Arg[1]-Pro[2]-Pro[3]-Gly[4]-Phe[5]-Ser[6]-Pro[7]-Phe[8]-Arg[9], produced from its precursor kininogen by the action of a group of proteases, called kallikreins. The peptide hormone is released in response to inflammation, trauma, burns, shock, allergy and some cardiovascular diseases, influencing vascular tone and permeability and decreasing blood pressure. Once released, BK initiates or enhances the release of mediators from leukocytes, stimulating the nociceptive afferent nerve terminals[1–5] and eliciting many pathophysiological responses, including septic and haemorrhagic shock, anaphylaxis, arthritis, rhinitis, asthma, inflammatory bowel disease, and certain other conditions including acute pancreatitis, post-gastrectomy dumping syndrome, carcinoid syndrome, migraine and hereditary angioedema.[1–9] Because of these dramatic activities, BK has been intensely studied for many years with the long-term vision of developing potential therapeutic agents which could act as competitive antagonists.

Since the first synthesis of BK in the laboratory in the early sixties,[10] a great effort has been invested in finding peptide analogs with antagonistic profile. A key sequence alteration was the replacement of Pro[7] in the native hormone by D-Phe. Although this analogue exhibits a weak agonist profile, it soon led to the discovery of the first BK antagonists. One of the best analogs reported of this generation was D-Arg-[Hyp[3], Thi[5,8], D-Phe[7]]-BK (NPC349), where Hyp stands for hydroxyproline and Thi for thienylalanine.[11] Subsequent suggestion that the C-terminus of BK adopts a β-turn in its bound conformation, led to the synthesis of

Key words: Bradykinin; B2 antagonists; bioactive conformation; conformational analysis; AMBER force field.
*Corresponding author.

0968-0896/98/$—see front matter
PII: S0968-0896(98)00084-4

conformationally constrained analogs. Thus, Knolle et al.[12] replaced the amino acids at positions 7 and 8 by D-Tic (tetrahydroisoquinoline carboxylic acid), and Oic (octahydroindole carboxylic acid), respectively, resulting in the design of the potent BK antagonist HOE-140, D-Arg-[Hyp^3, Thi^5, D-Tic^7, Oic^8]-BK.[13] In the same direction, Kyle et al.[14] replaced the proline at position 7 by hydroxyproline ethers and the phenylalanine at position 8 by Oic, providing one of the most active compounds, NPC17761 that contains D-*trans*-4-phenylthioproline at position 7. Both HOE-140 and NPC17761 are more potent than the earlier D-Phe7-containing antagonists. Recently, there have also been reported a few non-peptide analogs with limited activity.[15–17] In order to make a step further in the design of more potent, orally bioavailable BK antagonists, a deeper understanding of the bioactive conformation involved in antagonist receptor binding, together with a careful analysis of the large structure–activity relationship results available seems necessary.

Due to the difficulties associated with the achievement of a 3-D structure of the ligand–receptor complex, an indirect way to gather information about the bioactive form required for peptide antagonism is to perform a thorough analysis of the conformational properties of BK and its analogs. Both experimental and theoretical studies describing the conformational profile of BK and different analogs have been reported in the last years. Furthermore, experimental studies have been carried out in different environments and using diverse experimental techniques, including circular dichroism, electron spin resonance or NMR spectroscopy.[18–26] Results of these investigations, together with the information provided by different computational studies, indicated a common tendency of the peptides to adopt a β-turn conformation at their C-terminus, suggesting that this feature could be a requirement for ligand binding. Indeed, extensive molecular modeling[27–30] has convincingly demonstrated the presence of a β-turn stabilized by a hydrogen bond between the amide hydrogen of residue 9 and the carbonyl oxygen of residue 6, involving the four C-terminal residues of the potent antagonist HOE-140. In contrast, no secondary structure has clearly been identified at the N-terminus, confirmed by the lower pA2 values displayed by N-terminally cyclic analogs.[31,32]

The β-turn motif has been proposed in the literature as necessary condition for BK binding, but not as a sufficient one. Indeed, early structure–activity relationship studies indicated that binding affinity can be increased considerably when an arginyl residue is added to the N-terminus segment of BK analogs. This hypothesis was convincingly demonstrated by the design of the moderate antagonist pseudopeptide, NPC 18325,[33] where the stretch of residues from 2 to 5 in HOE140 is replaced by a 12-carbon chain. A recent study reporting the synthesis and in vitro evaluation of a series of small linear and cyclic peptides inspired on the C-terminal segment of second-generation BK antagonists, stressed once more, the importance of the C-terminus in BK antagonism.[34] This series of analogs provides new insights into the requirements for BK antagonism. Of these analogs, some exhibit a reasonable antagonistic profile at the B2 receptor. Due to their small size and rigid geometry, these peptides represent a suitable set to further assess the requirements of bradykinin antagonism. Consequently, in order to determine the chemical features, as well as their spatial arrangement, responsible for BK antagonism, we carried out an extensive conformational study on a selected subset of peptides of this series. From the analysis of the conformational profiles of these analogs a bioactive conformation is proposed. The analogs selected for the present study include three antagonists: cyclo-(Gly-Thi-D-Tic-Oic-Arg) (GTTOA), cyclo-(Gly-Ala-D-Tic-Oic-Arg) (GATOA) and cyclo-(Abu-Ala-Ser-D-Tic-Oic-Arg) (AASTOA) and two non-binders: cyclo-(Abu-D-Phe-Ala-D-Tic-Oic-Arg) (APATOA), and Thi-Ser-D-Tic-Oic-Arg (TSTOA). Table 1 lists the antagonist profile of these analogs as reported in ref 34.

The putative bioactive conformation of the selected BK antagonists was characterized in a two step procedure. First, a subset of conformations containing the low energy structures common to the active peptides was created. Second, structures from this set were systematically compared with the low energy conformations of non-binders, in order to find those conformations common to the active peptides that are at the same time not attainable by the non-binders. Following this procedure, two conformations were finally kept and considered as possible candidates for the bioactive conformation. Differences between the two candidates could be determined by analyzing the conformational profile of the highly potent BK antagonist HOE-140, computed in an independent study.[30] Systematic comparison of the two candidate conformations with the set of low energy conformations of HOE-140, helped us to propose a hypothesis concerning the stereo chemical requirements involved in BK antagonism as explained below.

Table 1. Pharmacological profile of the BK antagonists selected for the present study

		pA2
GTTOA	Gly-Thi-D-Tic-Oic-Arg	7.39 ± 0.24
GATOA	Gly-Ala-D-Tic-Oic-Arg	6.62 ± 0.46
AASTOA	Abu-Ala-Ser-D-Tic-Oic-Arg	6.51 ± 0.29
APATOA	Abu-D-Phe-Ala-D-Tic-Oic-Arg	inactive
TSTOA	Thi-Ser-D-Tic-Oic-Arg	inactive

Methods

All the calculations were carried out within the molecular mechanics framework using the all-atom AMBER 4.0 force field.[35] The peptides were studied in its zwitterionic form. The unnatural amino acid residues Thi, Tic, Oic, D-Phe and Abu (amino butyric acid) were constructed using the PREP module of AMBER. Partial charges for these residues were generated by fitting the molecular electrostatic potential produced with a STO-3G basis set using the GAUSSIAN94 suite of programs.[36] No explicit solvent was included in the calculations, although an effective dielectric constant of 80 was used to screen the electrostatic interactions and no cutoff was used.

The conformational space of the peptides was sampled using simulated annealing (SA) in an iterative fashion. The method has been described elsewhere.[37] The procedure requires a starting structure that is subjected to an annealing process and then minimized. This is the starting structure for a new cycle of SA after the molecule is abruptly heated. The procedure is repeated until a certain convergence criterium is fulfilled. Although some of the peptides studied in the present work are cyclic, generation of starting geometries do not represent a problem. In this case, geometries are also generated in an open extended conformation, and in parallel, information concerning their cyclic nature is stored in their respective topology files (these files contain information of the atoms actually bonded). When the structures are subjected to minimization, become cyclic within a few iterations of the energy optimization process.

For every peptide, the starting structure was energy minimized using the conjugate gradient algorithm, with a gradient convergence criterium set to 0.001 kcal/molÅ. Subsequently, the structure was heated up to 900 K at a rate of 100 K/ps. Heating is fast in order to force the molecule to jump to a different region of the conformational space. At this point the structure was cooled up to 200 K at a rate of 7 K/ps and then minimized. The structure was stored on a file and used as the starting conformation for a new cycle of SA. In this way, a library of low energy conformations was generated. These structures were rank ordered by energy every 100 cycles and checked for uniqueness. The procedure was repeated until no new conformations, excluding those that are local reoptimizations of the side chains appeared after a predetermined number of cycles within a 5 kcal/mol energy range with respect to the lowest energy structure already found.

As mentioned before, every 100 cycles the new structures obtained were added to a master list of unique conformations. In order to reject from the list those structures that were not unique, they were first rank ordered and analyzed for uniqueness in ascending energy order. A conformation was considered unique if at least one of the backbone dihedral angles, excluding those situated at both termini was different from 60° with respect to the previous conformations already on the list.

The conformational analysis of each peptide was carried out on the subset of unique conformations within a 5 kcal/mol threshold in respect to its global minimum. In order to facilitate the description of the preferred conformational domains exhibited by each peptide, the conformations of each low energy subsets were clustered into classes according to the values of the root mean square (rms) deviation of the distance between the backbone atom coordinates of every pair of structures, after they had been optimally superimposed. Since the use of the rms as similarity criterium requires to select a threshold value depending on the number of atoms compared,[38] a value of 0.65 Å was used for the two cyclic pentapeptides (GTTOA, GATOA) and a value of 0.83 Å was considered for the two cyclic hexapeptides (APATOA and AASTOA). For the linear pentapeptide TSTOA, a higher value of rms (0.90 Å) was selected, due to the contribute of both termini that does not need to be considered in the visual evaluation in order to consider two backbone conformations being the same.

Finally, computation of the rms deviation of the appropriate subset of backbone atoms was performed to carry out pairwise cross comparisons between conformations of the low energy subsets within the 5 kcal/mol threshold of the different analogs, in order to distinguish common conformations among them. After testing different threshold values by visual inspection, two conformations were considered similar if the rms difference value between the backbone atoms of the last four residues of the five peptides was lower or equal to 0.53 Å.

Results and Discussion

Exploration of the conformational space of the five analogs selected for the present study was carried out with the peptides in their zwitterionic form using a dielectric constant of 80, without explicit consideration of the solvent molecules. This methodology represents, at the present time, an unavoidable approximation if thorough explorations of the conformational space are required. Calculations carried out on model peptides, reveal that minima obtained using this procedure do not deviate much from the reminimized structures after the peptide is immersed in a box with solvent molecules.[39] Moreover, the small differences observed in the

Table 2. Results from the conformational analysis of the selected BK antagonists

	♯SA cycles	unique (angles)	ΔE less threshold	unique (rmsd)	global min
GTTOA	800	23	15	11	178
GATOA	900	19	13	9	53
AASTOA	2600	62	37	8	796
APATOA	1200	30	18	6	671
TSTOA	3200	438	111	50	1223

structures after reminimization lie inside the tolerances used in this work to classify peptide conformations into classes and consequently, these small deviations do not constitute a major drawback of the present exploratory procedure. However, it is possible that the relative order of energies of the different minima characterized, changes when solvation is accounted for explicitly. In this case the relative order of the low energy minima may change due to the different exposure of the conformations to the solvent. It is for this reason that values of the conformational energies should be used only as an indication and very cautiously.

Conformational analysis of the BK antagonists

The computational results regarding each of the peptides studied in the present work are schematically listed in Table 2. However, a more complete description of these results is provided below.

GTTOA

The sampling procedure was completed after 800 cycles of the iterative simulated annealing process. Of these conformations, 23 were considered unique following the criterium described in the methods section, being 15 of them within the 5 kcal/mol threshold above the global minimum. The lowest energy conformation was obtained at iteration number 178 with an energy of 11 kcal/mol. After calculation of all pairwise rms deviations as explained in the methods section, the subset of low energy unique structures within a 5 kcal/mol threshold, was reduced to 11 classes. Backbone dihedral angles of the representative conformation of each class (i.e. the conformation with the lower conformational energy in the class) are listed in Table 3. Analysis of the results reveals the propensity of the peptide to adopt bent type conformations. Furthermore, only the representative conformations of classes IV, VI, VIII and X show standard motives stabilized by hydrogen bonds. Specifically, the representative conformations of class IV and VI exhibit a γ-turn stabilized by a hydrogen bond between the amide hydrogen of Arg5 and the carbonyl oxygen of Tic3 and between the amide hydrogen of Thi2 and the carbonyl oxygen of Arg5, respectively, while the representative conformations of classes VIII and X show a β-turn stabilized by a hydrogen bond between the amide hydrogen of Gly1 and the carbonyl oxygen of Tic3 and two γ-turns between the amide hydrogen of Gly1 and the carbonyl oxygen of Oic4 and between the amide hydrogen of Thi2 and the carbonyl oxygen of Arg5, respectively. Due to the cyclic nature of the peptide, standard turns stabilizing the representative conformations of classes VI, VIII and X can be also interpreted as large cyclic structures of 14, 11 and 14 atoms, respectively. Although all low energy conformations appear predominantly as globular structures with no standard turns on them, a detailed analysis of Table 3 permits to identify βII′-turn motives not stabilized by hydrogen bonds involving the residues Thi2 and Arg5 in all the representative conformations, excluding those of classes I, IV, and IX. Similarly, βII-turns not stabilized by a hydrogen bond involving residues Gly1 and Oic4, have also been found in the representative conformations of classes VII, X, and XI.

Table 3. Backbone dihedral angles (in degrees) and relative conformational energies, ΔE (in kcal/mol) of the representative conformations of each of the 11 different classes found by iterative SA calculations of GTTOA

Class	I	II	III	IV	V	VI	VII	VIII	IX	X	XI
ΔE	0.0	2.0	3.1	3.4	3.7	3.9	4.0	4.0	4.3	4.4	4.5
ψ_1	−45	33	124	−55	125	−58	−63	−75	88	−79	−93
ω_1	−177	180	−179	178	−175	176	172	179	180	171	177
ϕ_2	−141	−162	64	−145	54	−147	−93	−126	68	−75	−75
ψ_2	55	70	85	51	69	108	121	84	65	124	116
ω_2	−170	−165	−176	−165	−164	180	−179	−154	179	−164	−163
ϕ_3	114	73	81	108	87	89	84	88	115	48	
ψ_3	−69	−115	−127	−73	−142	−112	−140	−146	−80	−139	−136
ω_3	175	161	169	178	178	176	176	−179	172	179	171
ϕ_4	−59	−52	−51	−75	−54	−53	−51	−50	−54	−56	−56
ψ_4	−35	120	114	39	122	−32	−53	107	33	−62	120
ω_4	−176	−177	−174	−176	179	−176	178	174	−176	−179	180
ϕ_5	178	79	61	75	48	173	−75	62	166	−77	73

Table 4. Backbone dihedral angles (in degrees) and relative conformational energies, ΔE (in kcal/mol) of the representative conformations of each of the nine different classes found by iterative SA calculations of GATOA

Class	I	II	III	IV	V	VI	VII	VIII	IX
ΔE	0.0	2.3	2.3	2.5	3.1	3.7	3.9	5.0	
ψ_1	−55	136	97	124	−47	−63	−79	−55	87
ω_1	−179	−179	−178	−175	−179	179	178	173	−173
ϕ_2	−138	57	63	51	−119	−129	−121	−98	65
ψ_2	64	80	65	70	98	89	86	115	61
ω_2	−174	−170	176	−162	−173	−173	−155	−176	180
ϕ_3	115	86	117	85	79	83	87	86	111
ψ_3	−71	−142	−79	−144	−129	−120	−145	−142	−91
ω_3	175	173	175	−178	163	171	−179	176	−177
ϕ_4	−59	−48	−59	−52	−50	−60	−51	−53	−54
ψ_4	−35	122	−38	118	116	76	108	−46	−42
ω_4	−176	−172	−175	179	−175	177	174	176	−176
ϕ_5	179	67	−179	50	77	79	61	−72	166

GATOA

After 900 cycles of simulated annealing, only 19 conformations were characterized as unique. Of these conformations, 13 were in the low energy subset with energies up to 5 kcal/mol above the global minimum. The lowest energy conformation was obtained at iteration number 53 and its energy is 9.2 kcal/mol. Conformations were clustered in nine classes after computation of the rms deviation of the backbone atom coordinates between every pair of structures as explained in the methods section. All the conformations, excluding only one (the representative conformation of class VI) exhibit a bent structure with no standard turns stabilized by a hydrogen bond. Backbone dihedral angles of the representative conformations of the nine classes found for GATOA are listed in Table 4. Specifically, the representative conformation of class VI shows two γ-turns stabilized by a hydrogen bond between the amide hydrogen of Arg5 and the carbonyl oxygen of Tic3 and between the amide hydrogen of Ala2 and the carbonyl oxygen of Arg5 (also a C14, considering the other path of the cyclic structure), respectively. Most of the conformational classes of this peptide exhibit a βII′-turn, not stabilized by a hydrogen bond and involving the C-terminal segment of the peptide. Only the representative conformations of classes I, III and IX do not exhibit this conformational motif. Moreover, the residues Gly1 and Oic4 are also involved in βI′- and βII-turns not stabilized by hydrogen bonds. Specifically, the representative conformations of classes II, III, IV and IX present a βI′-turn, while that representative of class VIII show a βII-turn.

AASTOA

The exploration of the conformational space of this cyclic peptide was completed after 2600 cycles of simulated annealing. After completion of this procedure, 62 unique conformations were characterized. Of these, 37 structures were within a 5 kcal/mol threshold above the global minimum. The lowest energy conformation was obtained at iteration number 796 with an energy of 14.6 kcal/mol. The structures were subsequently clustered using the values of the rms deviation of the backbone atom coordinates of each pair of structures computed after optimal superimposition. Following this procedure the low energy structures were classified into eight classes and the backbone dihedral angles of the representative conformations of each class are shown in Table 5. The peptide exhibits a tendency to adopt bent conformations, although β-turns, not stabilized by hydrogen bonds, are found at both termini. Specifically,

Table 5. Backbone dihedral angles (in degrees) and relative conformational energies, ΔE (in kcal/mol) of the representative conformations of each of the eight different classes found by iterative SA calculations of AASTOA

Class	I	II	III	IV	V	VI	VII	VIII
ΔE	0.0	0.4	0.6	0.9	1.3	2.2	2.4	3.4
ψ_1	70	163	154	152	65	68	161	83
ω_1	2	1	2	1	1	0	2	2
ϕ_2	−143	−99	−95	−86	−134	−130	−74	−67
ψ_2	121	−136	−70	−67	169	−76	176	−54
ω_2	180	−174	−174	−176	180	178	179	180
ϕ_3	68	45	−42	−76	52	−66	48	−153
ψ_3	63	62	109	145	59	119	79	164
ω_3	−178	−169	178	−175	−179	−177	166	−174
ϕ_4	117	64	80	137	104	80	79	69
ψ_4	−69	−131	−140	−63	−93	−137	−123	−123
ω_4	176	175	172	−2	172	175	−177	163
ϕ_5	−55	−52	−55	−62	−58	−55	−46	−55
ψ_5	−30	130	−62	135	104	148	−27	105
ω_5	−177	179	177	−178	−177	178	−178	−179
ϕ_6	177	165	44	−77	83	83	−54	82

all the representative conformations of the selected eight classes, excluding those representative of the classes I, IV and V, exhibit βII′-turns involving the residues Arg6 and Ser3, while the representative conformations of classes III and IV show βIII-turns involving the residues Abu1 and Tic4 and that representative of class VII present a βII-turn involving the same N-terminal part. The only motives stabilized by hydrogen bonds are a α-turn between the amide hydrogen of Arg6 and the carbonyl oxygen of Ala2 found in the representative conformation of class IV, and a C8 or C16 cycle between the amide hydrogen of Abu1 and the carbonyl oxygen of Ala2 found in the representative conformation of class VIII.

APATOA

The sampling procedure required, in this case, 1200 cycles of simulated annealing yielding 30 unique conformations. Of these, 18 lie within a threshold of 5 kcal/mol above the global minimum. The global minimum was obtained at iteration number 671, exhibiting an energy of 14.8 kcal/mol. Computation of the rms deviation of the backbone atom coordinates between every pair of structures after optimal superimposition provided six classes of conformations. Backbone dihedral angles of these six classes are listed in Table 6. The conformational profile of the peptide exhibits a high tendency to adopt bent conformations with the only presence of a βII′-turn stabilized by a hydrogen bond between the amide hydrogen of Arg6 and the carbonyl oxygen of Ala3, as found in the representative conformation of class II. Other standard motives, not stabilized by hydrogen bonds, can also found. Specifically, all the representative conformations of the six classes, excluding that of class V, exhibit βII′-turns involving the residues Arg6 and Ala3, while only the representative conformation of class III show a βIII-turn motif at the N-terminus involving the residues Abu1 and Tic4.

Table 6. Backbone dihedral angles (in degrees) and relative conformational energies, ΔE (in kcal/mol) of the representative conformations of each of the 6 different classes found by iterative SA calculations of APATOA

Class	I	II	III	IV	V	VI
ΔE	0.0	1.1	1.4	1.6	4.0	4.2
ψ_1	133	92	82	136	132	−51
ω_1	−2	−1	−2	0	−4	0
ϕ_2	75	78	84	74	75	108
ψ_2	−153	−147	55	−117	−154	−46
ω_2	−178	180	178	178	−179	177
ϕ_3	−125	−114	48	−147	−145	−146
ψ_3	103	108	76	−54	66	65
ω_3	−175	178	−172	1	−160	−159
ϕ_4	80	79	76	104	109	61
ψ_4	−111	−128	−140	−157	−79	−144
ω_4	161	171	173	−165	−173	173
ϕ_5	−54	−63	−55	−61	−61	−54
ψ_5	157	−3	128	−61	−63	125
ω_5	180	−173	−177	−176	−170	−178
ϕ_6	112	−46	155	−53	−59	71

TSTOA

After 3200 cycles of simulated annealing, 438 conformations were characterized as unique. Of these conformations, 111 were in the low energy subset with energies up to 5 kcal/mol above the global minimum. The lowest energy conformation was obtained at iteration number 1223 and its energy is 4.1 kcal/mol. The structures were subsequently clustered into 50 classes from the values of the rms deviation between the backbone atom coordinates of each pair of structures after optimal superimposition. Backbone dihedral angles of the 50 classes are listed in Table 7. Analysis of the low energy conformations reveals a high tendency of the peptide to adopt bent conformations. Of the 50 representative conformations, only eight present motives stabilized by hydrogen bonds. Specifically, the representative conformations of classes XIV and XXXII exhibit an α-turn motif stabilized by a hydrogen bond between the amide hydrogen of Arg5 and the carbonyl oxygen of Thi1; the representative conformations of classes XXXIX, ILIV and ILVI present βII′-turn motif stabilized by a hydrogen bond between the amide hydrogen of Arg5 and the carbonyl oxygen of Ser2; the representative conformations of classes XXXV, and IL show a C14 cyclic structure stabilized by a hydrogen bond between the amide hydrogen of Ser2 and the carbonyl oxygen of Arg5; finally, the representative conformation of class ILIX exhibit a βII′-turn motif stabilized by a hydrogen bond between the amide hydrogen of Arg5 and the carbonyl oxygen of Tic3. Moreover, a detailed analysis of Table 7 permits to establish the presence of β-turns not stabilized by hydrogen bonds at the C- and N-terminus of the peptide sequence. In contrast to the studied cyclic peptides, only the 50% of the representative conformations of the 50 selected classes, show a βII′-turn motif not stabilized by a hydrogen bond. βII-, βI′- and βIII′-turns are also present at the N-terminus, involving the residues Thi1 and Oic4.

Characterization of the bioactive conformation

In order to characterize the bioactive conformation responsible of BK B2 antagonism, it is necessary to perform cross comparisons between the sets of low energy conformations of the different analogs studied. The bioactive conformation needs to be common to the antagonists and at the same time has not to be found in any of the nonbinder sets of conformations. Sets of unique conformations generated in the present work

involve comparisons of backbone atoms or dihedrals. It could be argued that, since most of the ligand–receptor interactions occur via peptide side chains, these should be included in the structural comparisons. Indeed, side chains have low energy torsional barriers and they are capable of sampling the whole conformational space, limited by the conformations attainable by peptide backbones.[40] Obviously, if backbone conformations are similar, side chains will sample the same conformational space. However, sometimes backbones can be different and the side chains still sample common regions of their respective conformational space. This occurs when a residue is presumably involved in the interaction with its receptor and appears in different position in different analogs, in such a case comparison between side chains becomes necessary.[41] However, in the cases where peptide analogs have similar sequences, like in the present study, is enough to carry out comparisons of peptide backbones.

Table 7. Backbone dihedral angles (in degrees) and relative conformational energies, ΔE (in kcal/mol) of the representative conformations of each of the 50 different classes found by iterative SA calculations of TSTOA

Class	I	II	III	IV	V	VI	VII	VIII	IX	X	XI	XII	XIII	XIV	XV	XVI	XVII
ΔE	0.0	0.4	0.7	1.2	1.3	1.6	1.8	2.0	2.0	2.0	2.1	2.2	2,2	2.2	2.3	2.3	2.4
ψ_1	−34	97	−174	−66	−48	163	−49	−11	120	−49	−73	153	83	−59	159	161	100
ω_1	176	−179	−179	180	−178	179	178	179	177	180	180	−179	−179	180	177	−179	
ϕ_2	−145	−123	−53	−78	−116	−130	−149	−65	52	42	−164	−139	−115	−70	−130	−134	−161
ψ_2	82	95	117	138	70	61	58	73	78	57	65	154	129	98	63	148	
ω_2	175	−174	−176	−175	−171	−171	−172	−165	−3	−179	−167	−177	175	−167	−174	−173	−175
ϕ_3	78	80	84	110	118	118	107	104	86	74	112	125	93	107	79	122	114
ψ_3	−141	−137	−122	−74	−66	−62	−85	−82	−142	−148	−70	−60	−136	−77	−135	−73	
ω_3	175	171	175	−179	179	177	163	179	178	175	165	−179	178	173	178	−174	180
ϕ_4	−51	−51	−52	−50	−52	−57	−54	−49	−46	−57	−54	−49	−52	−49	−48	−49	−53
ψ_4	−41	−48	148	−53	−44	165	126	133	−46	−54	123	−46	139	−44	143	−54	−51
ω_4	180	179	180	179	179	178	−177	−179	178	−175	179	180	179	−179	−176	179	
ϕ_5	−70	−164	−72	−68	−66	−85	−72	−109	−76	−166	64	−134	−92	−154	−76	60	−70

Class	XVIII	XIX	XX	XXI	XXII	XXIII	XXIV	XXV	XXVI	XXVII	XXVIII	XXIX	XXX	XXXI	XXXII	XXXIII	XXXIV
ΔE	2.4	2.5	2.6	2.6	2.7	2.7	2.7	2.8	3.1	3.3	3.5	3.6	3.7	3.8	3.8	3.8	3.8
ψ_1	−61	122	135	148	139	−15	104	141	−60	142	−59	−73	−160	−71	142	74	133
ω_1	180	180	179	180	180	180	179	180	176	173	−175	−179	180	179	179	−179	−179
ϕ_2	62	−155	−59	−161	−62	−155	44	41	40	−158	69	−63	−108	−58	−114	−161	−78
ψ_2	67	100	142	−59	129	152	56	77	80	161	63	120	88	−58	104	142	148
ω_2	176	−3	−163	178	−176	176	−175	170	175	−175	−178	−167	3	178	−2	171	174
ϕ_3	128	74	100	133	87	92	105	81	72	−38	120	101	127	88	87	92	
ψ_3	−60	−145	−103	−54	−123	−141	−87	−143	−134	−58	−66	−85	−56	−55	−138	−137	−122
ω_3	179	178	−7	178	172	171	180	−178	175	178	175	−174	178	178	−3	180	176
ϕ_4	−48	−56	−60	−47	−50	−50	−56	−52	−52	−51	−60	−53	−47	−48	−60	−48	−44
ψ_4	−46	148	158	−45	−135	−36	151	−38	141	−48	178	−65	−46	−44	122	−48	−48
ω_4	−179	179	180	176	−178	179	178	−178	−179	177	−176	179	177	−176	180	176	
ϕ_5	−156	−162	−150	−63	62	−67	−92	−67	−157	−71	−128	55	−67	−63	−79	58	59

Class	XXXV	XXXVI	XXXVII	XXXVIII	XXXIX	XL	XLI	XLII	XLIII	XLIV	XLV	XLVI	XLVII	XLVIII	XLIX	L
ΔE	3.8	4.0	4.0	4.3	4.4	4.5	4.6	4.6	4.6	4.6	4.7	4.7	4.8	4.9	4.9	5.0
ψ_1	123	−68	168	143	−59	−60	138	−56	168	133	86	106	165	148	43	88
ω_1	−175	178	177	180	−179	179	−176	180	179	180	180	−177	−177	−179	179	−178
ϕ_2	−148	−154	−131	60	178	−173	−158	−81	−69	50	53	−63	−135	43	−77	−128
ψ_2	95	77	63	81	78	150	96	155	−64	68	78	−75	103	62	124	59
ω_2	180	175	−175	−3	−178	174	174	−179	−173	−170	180	−168	−4	−163	−166	−165
ϕ_3	73	77	122	81	−36	90	73	129	122	−35	77	112	89	−30	104	120
ψ_3	−141	−145	−59	−135	−57	−140	−142	−64	−68	−56	−134	−74	−140	−62	−72	−71
ω_3	172	−177	172	173	179	173	173	−2	175	179	171	171	6	177	171	−1
ϕ_4	−58	−53	−52	−51	−50	−48	−53	−66	−53	−47	−53	−48	−60	−51	−66	−63
ψ_4	104	122	113	145	−45	−42	−44	163	123	−46	162	−55	−65	101	72	156
ω_4	−179	179	−176	179	178	176	180	174	−179	177	−179	176	−178	−179	−178	180
ϕ_5	62	−95	−156	−85	−68	−132	−66	−137	−139	−77	80	−165	−106	−142	−161	−70

In order to carry out similarity measures on the sets of conformations characterized in the present study, it should be noticed that most of the analogs studied in the present work are five and six residue cyclic peptides. When comparing backbone conformations, the constrained nature of the cyclic structures, makes impossible to find any similarity if comparisons are performed on the whole structures. Systematic comparison of the different structures failed to provide common positions of any but a set of residues ultimately considered in similarity measures in the present work. Structure–activity studies suggest that the last three residues, that are identical in all the analogs studied in the present work, are important for B2 BK antagonism and should be included.[34] On the other hand, these cyclic analogs exhibit conformations that are close to β-turn secondary structures as it had been postulated for BK antagonists.[18–30] Since these secondary structure motifs involve four residues, conformations in this work were compared by their last four residue segments. This criterion can be considered as minimum requirements for recognition, although does not necessarily rule out the possible steric moludation of the residues not included.

In order to characterize prospective candidates to be the bioactive conformation, the initial sets of low energy conformations of each peptide analogue characterized before the rmsd pruning, and within a certain energy threshold were considered. Specifically, the subset of low energy conformations within a 5 kcal/mol threshold of the more active analogue GTTOA, was compared with those of the other two antagonists: GATOA and AASTOA. Pairwise comparisons of the low energy conformations of the three peptides allowed to discard 10 conformations of GTTOA as prospective candidates to be the bioactive conformation. In a further step, the subset of low energy conformations common to the three antagonists was pairwisely compared for similarity with the low energy conformations of the two non-binders: APATOA and TSTOA. Pairwise comparison of the low energy conformations common to the three active peptides with those of the two inactive conformations yielded two structures of GTTOA candidates to be the bioactive conformations. Rms deviation between backbone atoms of the two conformations after optimal superimposition is 0.45 Å, lower than the threshold value of 0.65 Å used to classify two conformations as different. This result owed us to consider the two conformations as being the same regarding their backbone. In this analysis the most similar conformation of GATOA exhibited a rms deviation of 0.06 Å and 0.31 Å for the most similar conformation of GTTOA. In contrast, the most similar conformations of TSTOA and APATOA were 0.57 Å and 0.80 Å, respectively.

Superimposition of the two putative bioactive conformations is illustrated in Figure 1. Visual inspection of the two conformations shows that the only critical difference between them, lies on the different orientation of the vector Cβ-Cγ on the Arg5 side chain. The orientation of this residue is important since the guanidinium moiety is putatively involved in peptide recognition.[16,33] In order to decide which of the two orientations was a better candidate to be the bioactive conformation, the two conformations selected were superimposed with all the low energy conformations of HOE-140, that had been characterized in an independent study in our laboratory.[30] Figure 2 shows the two conformations of GTTOA (green and orange) with the conformation of HOE-140 (red) that exhibits the lowest rms deviation value (0.95 Å) comparing only the backbone atoms. The figure clearly shows that one of the candidates exhibits the vector Cβ-Cγ on residue Arg5 pointing in the same direction of Arg9 in HOE-140 (downwards in regard to the cycle), whereas in the other candidate the vector points in the opposite direction (upwards in regard to the cycle). On the other hand, the non-binder TSTOA (blue) exhibits the arginyl side chain in all the conformations characterized pointing in the same direction of Arg9 in HOE-140. Inspection of Figure 2 suggests that the arginyl residues located at the N-terminus in HOE-140 lie above the cycle, in the same spatial region of the arginyl residue of the cyclic analogue. This leads to the hypothesis that the bioactive conformation exhibits the arginyl side chain above the cycle and this role is played by the N-terminal residues in HOE-140. This hypothesis explains at the same time the lack of affinity exhibited by the linear analogue TSTOA since in this case there are no extra arginyl residues at the N-terminus and the analogue cannot comply the requirements of the bioactive conformation, as HOE-140 does.

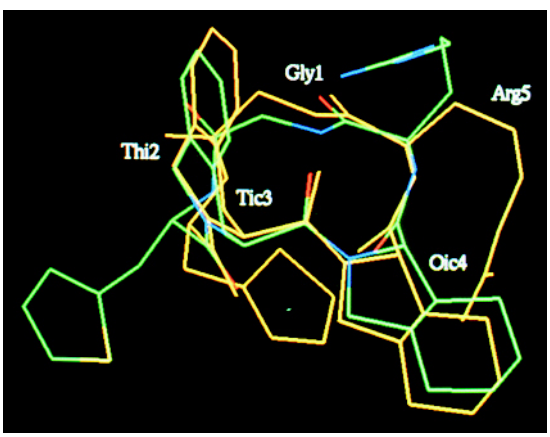

Figure 1. Superimposition of the two low energy conformations of GTTOA candidates to be the bioactive conformation.

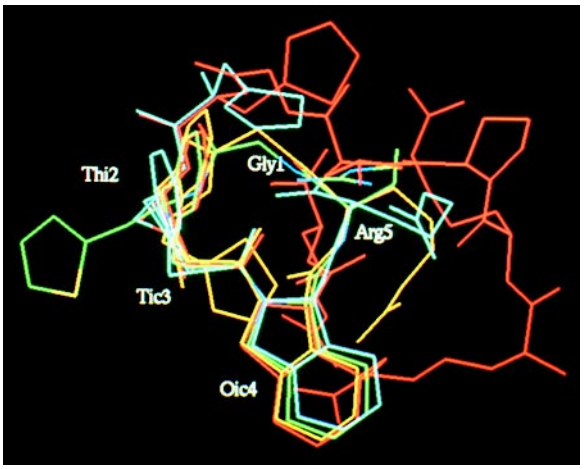

Figure 2. Superimposition of the two low energy conformations of GTTOA candidates to be the bioactive conformation (in green and orange, respectively), together with the most similar conformation of HOE-140 (red) and TSTOA (blue).

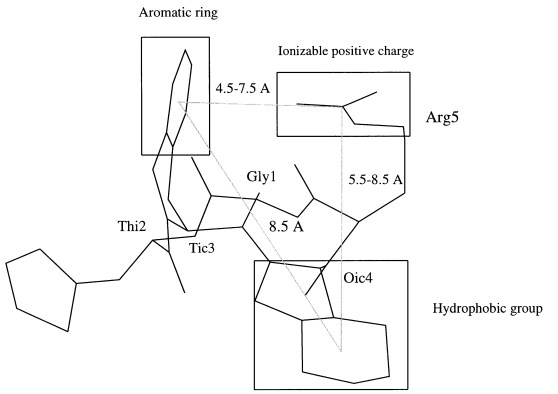

Figure 3. Proposed pharmacophore for antagonism to the bradykinin B2 receptor.

Proposal of a pharmacophore for the BK antagonism

Knowledge of the bioactive conformation responsible of BK antagonism together with the information available from different structure activity studies, give the opportunity to propose a pharmacophore where, ligand–receptor interactions are described in terms of the chemical moieties involved in their three-dimensional arrangement. Structure–activity relationship studies suggest that the side chains of the three residues common to all analogs studied in the present work: Tic, Oic and Arg, are involved in the interaction with the receptor.[34] The aromatic ring of Tic is probably involved on a $\pi - \pi$ interaction; residue Oic can only be involved in a hydrophobic interaction; and the guanidinium group of the arginyl residue is probably involved in a charge–charge interaction with the receptor. This hypothesis can also be indirectly corroborated by different results from site-directed mutagenesis experiments. These studies have demonstrated a deleterious effect on ligand binding of mutations on the B2 bradykinin receptor at positions $Phe^{261\ 42}$ and $Asp^{268\ 43}$ both located on transmembrane VI. Accordingly, the aspartic acid could be involved in an interaction with the charged moiety of the guanidinium group and on the other hand, the phenylalanine with either an aromatic moiety or simply with a hydrophobic group of the ligand. In summary, the groups describing schematically the pharmacophore are: an aromatic group, a hydrophobic moiety and an ionizable positive charge. Regarding their spatial arrangement, since the pharmacophore has only three points, the spatial arrangement of the group can be specified by three geometrical parameters, for example the distances between them. The distance between the aromatic ring and the hydrophobic moiety exhibits a low tolerance due to their conformational constraints. However, distances from these two moieties to the positive charge are less precise, due to the flexible nature of the arginyl side chain and the procedure used in the present work to assess the bioactive conformation, based on a detailed analysis of peptide backbones. Figure 3 shows schematically the descriptors of the pharmacophore indicating the chemical moieties involved as well as their spatial arrangement.

It is expected that these results are helpful for designing a third generation of BK no-peptide antagonists. Work in this direction is presently being undertaken in our laboratory.

Conclusions

The conformational profiles of five BK analogs was assessed by computational methods. The set of analogs selected for the present study included three antagonists and two nonbinders. The analogs selected were taken from a recent study of BK analogs inspired in the C-terminus region of the potent second generation antagonists represented by HOE-140 and NPC17761. The conformational energy was computed using molecular mechanics and exploration of the conformational space was performed using simulated annealing in an iterative fashion. Comparison of the common conformations among antagonists and at the same time not found in the non-binders provided a putative bioactive conformation. These results, together with the structure–activity relationship studies published in the literature, were used to propose a pharmacophore for BK antagonism that includes an ionizable positive charge, a hydrophobic group and an aromatic (hydrophobic) group in a specific spatial arrangement shown in Figure 3.

Acknowledgements

This research was partially supported by the Ministerio de Cultura y Educacion through the CICYT under contract PTR94-0150. We are also grateful to the Human Capital and Mobility program 'Access to Large Installations', under contract CHGE-CT92-0009 between The European Community and CESCA/CEPBA.

References

1. Clark, W. G. In *Handbook of Experimental Pharmacology*; Erdos, E. G., Ed.; Springer-Verlag: New York, **1979**; Vol. XXV, pp 311–56.

2. Marcenau, F.; Lussier, A.; Regoli, D.; Giroud, J. F. *Gen. Pharmacol.* **1983**, *14*, 209.

3. Taiwo, Y. O.; Levine, J. D. *Brain Res.* **1988**, *458*, 402.

4. Steranka, L. R.; Manning, D. C.; DeHaas, C. J.; Ferkany, J. W.; Borosky, S. A.; Connor, J. R.; Vavrek, R. J.; Stewart, J. M.; Snyder, S. H. *Proc. Natl. Acad. Sci. U. S. A.* **1988**, *85*, 3245.

5. Dray, A.; Bettaney, J.; Forster, P.; Perkins, M. N. *Neurosci. Lett.* **1988**, *91*, 301.

6. Dray, A.; Perkins, M. *Trends Neur.* **1993**, *16*, 99.

7. Griesbacher, T.; Lembeck, F. *Br. J. Pharmacol.* **1987**, *92*, 333.

8. Steranka, L. R.; Farmer, S. G.; Burch, R. M. *FASEB J.* **1989**, *3*, 2019.

9. Haley, J. E.; Dickenson, A. H.; Schachter, M. *Neurosci. Lett.* **1989**, *97*, 198.

10. Boissonnas, R. A.; Guttmann, S.; Jaquenoud, P. A. *Helv. Chim. Acta.*, **1960**, *43*, 1349.

11. Vavrek, R. J.; Stewart, J. M. *Peptides* **1985**, *6*, 161.

12. Lembeck, F.; Griesbacher, T.; Eckhardt, M.; Henke, St.; Breipohl, G.; Knolle, J. *Br. J. Pharmacol.* **1991**, *102*, 297.

13. Wirth, K.; Hock, F. J.; Albus, U.; Linz, W.; Alpermann, H. G.; Anagnostopoulos, H.; Henke, S.; Breiphol, G.; König, W.; Knolle, J.; Schölkens, B. A. *Br. J. Pharmacol.* **1991**, *102*, 774.

14. Kyle, D. J.; Martin, J. A.; Burch, R. M. *J. Med. Chem.* **1991**, *34*, 2649

15. Calixto, J. B.; Yunes, R. A.; Rae, G. A.; Medeiros, Y. S. *Inflam. Dis. Ther.* **1990**, *5* 97.

16. Salvino, J. M.; Seoane, P. R.; Douty, B. D.; Awad, M. A.; Dolle, R. E.; Houck, W. T.; Faunce, D. M.; Sawutz, D. G. *J. Med. Chem.* **1993**, *36*, 2583.

17. Witherup, K. M.; Ransom, R. W.; Graham, A. C.; Bernard, A. M.; Salvatore, M. J.; Lumma, W. C.; Anderson, P. S.; Pitzenberger, S. M.; Varga, S. L. *J. Am. Chem. Soc.* **1995**, *11* 6682.

18. Lee, S. C.; Russell, A. F.; Laidig, W. D. *Int. J. Pept. Prot. Res.* **1990**, *35*, 367.

19. Kyle, D. J.; Hicks, R. P.; Blake, P. R.; Klimkowski, V. J. In *Bradykinin Antagonists: Basic and Clinical Research*; Burch R. M., Ed.; Marcel Dekker: New York, **1991**; pp 131–146.

20. Liu, X.; Stewart, J. M.; Gera, L.; Kotovych, G. *Biopolymers* **1993**, *33*, 1237.

21. Otter, A.; Bigler, P.; Stewart, J. M.; Kotovych, G. *Biopolymers* **1993**, *33*, 769.

22. Guba, W.; Haessner, R.; Breipohl, G.; Henke, S.; Knolle, J.; Santagada, V.; Kessler, H. *J. Am. Chem. Soc.* **1994**, *116* 7532.

23. Cann, J. R.; Liu, X.; Stewart; J. M.; Gera, L.; Kotovych, G. *Biopolymers* **1994**, *34*, 869.

24. Young, J. R.; Hicks, R. P. *Biopolymers* **1994**, *34*, 611.

25. Pellegrini, M.; Mammi, S.; Gobbo, M.; Rocchi, R.; Peggion, E. *Biopolymers* **1995**, *36*, 461.

26. Pellegrini, M.; Mammi, S.; Gobbo, M.; Rocchi, R.; Peggion, E.; Mierke, D. F. *Biopolymers* **1997**, *40*, 561.

27. Kyle, D. J.; Blake, P. R.; Smithwiok, D.; Green, L. M.; Martin, J. A.; Sinsko, J. A.; Summers, M. F. *J. Med. Chem.* **1993**, *36*, 1450.

28. Salvino, J. M.; Seoane, P. R.; Dolle, R. E. *J. Comp. Chem.* **1993**, *14*, 438.

29. Perez, J. J.; Sanchez, Y. M.; Centeno, N. B. *J. Pept. Sci.* **1995**, *1*, 227.

30. Filizola, M.; Boada, N.; Carteńi-Farina, M.; Perez, J. J. *J. Biomol. Struct. Dyn* **1997**, *15*, 639.

31. Chakravarty, S.; Wilkins, D.; Kyle, D. J. *J. Med. Chem.* **1993**, *36*, 2569.

32. Seyfarth, F.; Felipe Pineda De Castro, L.; Liepina, I.; Paegelow, I.; Liebmann, C.; Reissmann, S. *Int. J. Pept. Protein Res.* **1995**, *46*, 155.

33. Kyle, D. J.; Chakravarty, S.; Sinsko, J. A.; Stormann, T. M. *J. Med. Chem.* **1994**, *37*, 1347.

34. Thurieau, C.; Feleton, M.; Hennig, P.; Raimbaud, E.; Canet, E.; Fauchere, J.-L. *J. Med. Chem.* **1996**, *39*, 2095.

35. Pearlman, D. A.; Case, J. C.; Cadwell, J. C.; Seibel, G. L.; Singh, U. C.; Weiner, P.; Kollman, P. A. *AMBER4.0*, University of California, San Francisco, 1991.

36. Frisch, M. J.; Trucks, G. W.; Schlegel, H. B.; Gill, P. M. W.; Johnson, B. G.; Robb, M. A.; Cheeseman, J. R.; Keith, T.; Petersson, G. A.; Montgomery, J A.; Raghavachari, K.; Al-Laham, M. A.; Zakrzewski, V. G.; Ortiz, J. V.; Foresman, J. B.; Peng, C. Y.; Ayala, P. Y.; Chen, W.; Wong, M. W.; Andres, J. L.; Replogle, E. S.; Gomperts, R.; Martin, R. L.; Fox, J.; Binkley, J. S.; Defrees, D. J.; Baker, J.; Stewart, J. J. P.; Head-Gordon, M.; Gonzales, C.; Pople, J. A. *Gaussian 94, Revision B.2*, Gaussian Inc. Pittsburgh PA, 1995.

37. Filizola, M.; Centeno, N. B.; Perez, J. J. *J. Pept., Sci.* **1997**, *3*, 85.

38. Maiorou, V. N.; Crippen, G. M., *Proteins* **1995**, *22*, 273.

39. Perez, J. J.; Loew, G. H.; Villar, H. O. *Int. J. Quant. Chem.* **1992**, *44*, 263.

40. van der Spoel, D.; Berendsen, H. J. C. *Biophys. J.* **1997**, *72*, 2032.

41. Perez, J. J.; Villar, H. O.; Uyeno, E.; Toll, L.; Olsen, C.; Polgar, W.; Loew, G. H. *Int. J. Quant. Chem., QBS* **1993**, *20*, 147.

42. Freedman, R.; Jargin, K. *Agents Actions Suppl.* **1992**, *38*, 487.

43. Nardone, J.; Hogan, P. G. *Proc. Natl. Acad. Sci. U.S.A.* **1994**, *91*, 4417.